Elephant Moraine 87521, 96008

Basaltic or gabbroic (polymict) fragmental breccia

31, 53 g

Figure 1A: Photograph of Elephant Moraine (EET) 87521 taken at the Johnson Space Center in the Meteorite Processing Laboratory. Figure 1B: Photograph of EET 96008 taken at the Johnson Space Center in the Meteorite Processing Laboratory.

Introduction

On the 1987-1988 ANSMET expedition, a 31 g achondrite, EET 87521 (Fig. 1A), was discovered in the Elephant Moraine Icefield (EET), in a sub-region referred to as Meteorite City (Figs. 2 and 3). Initially, EET 87521 was classified as a eucrite, based on its texture and mineralogy. However, after more detailed study including determination of Fe/Mn, Ga/Al and O isotopic ratios, it was recognized as a lunar basaltic breccia and immediately reclassified (Delaney, 1989; Warren and Kallemeyn, 1989; Score and Lindstrom, 1990). This was the first meteorite discovered that was derived from a mare region on the Moon. Nine years later, in the 1996-1997 ANSMET season, another paired and larger (53 g) piece of this breccia was discovered in Meteorite City – EET 96008.

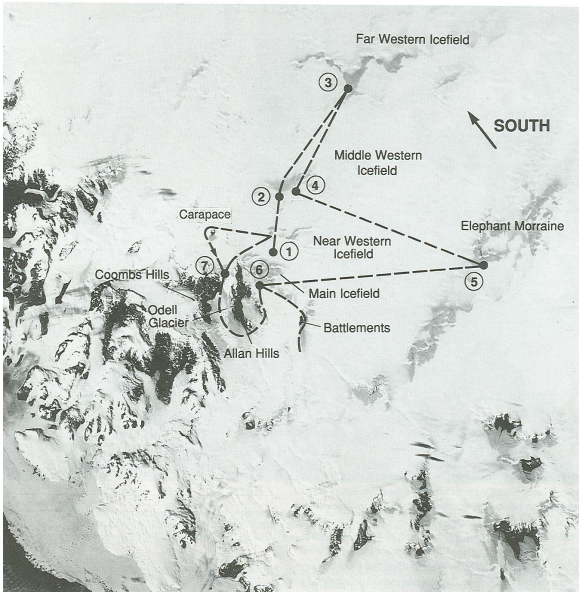

Figure 2: The Elephant Moraine icefield region, home of the EET series ANSMET meteorites.

Figure 3: Meteorite City region of the Elephant Moraine Icefield where EET 87521 and EET 96008 were discovered.

Petrography and Mineralogy

EET 87521 and EET 96008 are both basaltic regolith breccias that contain a diversity of clasts that have a mare affinity. Takeda et al. (1992) described basaltic, gabbroic and feldspathic basaltic clasts in section ,55. Warren and Kallemeyn (1989) found ophitic basalt clasts as well as some highlands material and impact melts in section ,9. Both Warren and Kallemeyn (1989) and Anand et al. (2003) estimate modes of approximately 80% brecciated matrix and 20% clasts for EET 87521 and EET 96008, respectively. Finally, Delaney (1989) reports 10% olivine, 47% subcalcic pyroxene, 38% calcic plagioclase, 4% silica and 1% of ilmenite, chromite, Ti-chromite and sulfide in section ,8.

Pyroxene compositions are variable and extend to very Fe-rich components (Fig. 6). Although there is plagioclase as sodic as An_{70}, the preponderance of feldspar compositions are near An_{90-92} (Figure 7). The range of spinel compositions in the EET basaltic meteorites spans nearly the entire range documented in Apollo lunar mare basalt suites, from Cr-rich spinel to Ti-chromites to ulvospinels (Fig. 8).

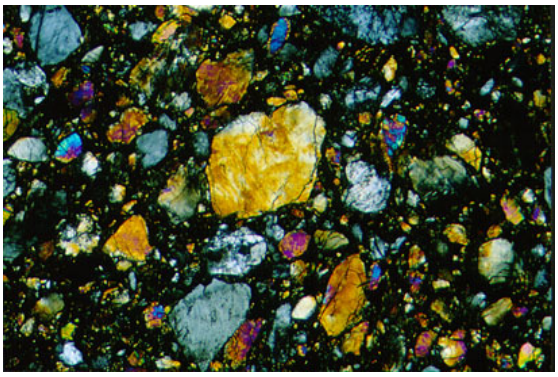

Figure 4: Photomicrograph of section ,4 of EET 87521, illustrating basaltic and highlands material.

Figure 5: Photomicrograph and sketch of section ,9 from the study of Warren and Kallemeyn (1989).

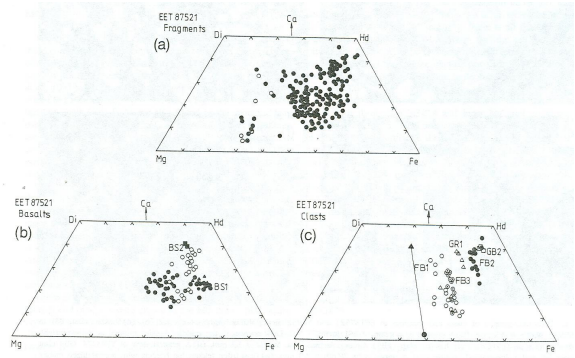

Figure 6: Pyroxene compositions from clasts and fragments in EET 87521 from Takeda et al. (1990).

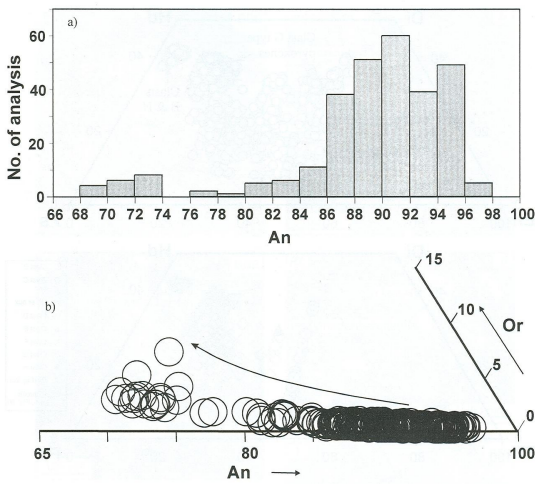

Figure 7: Plagioclase compositions for EET 96008 from Anand et al. (2004).

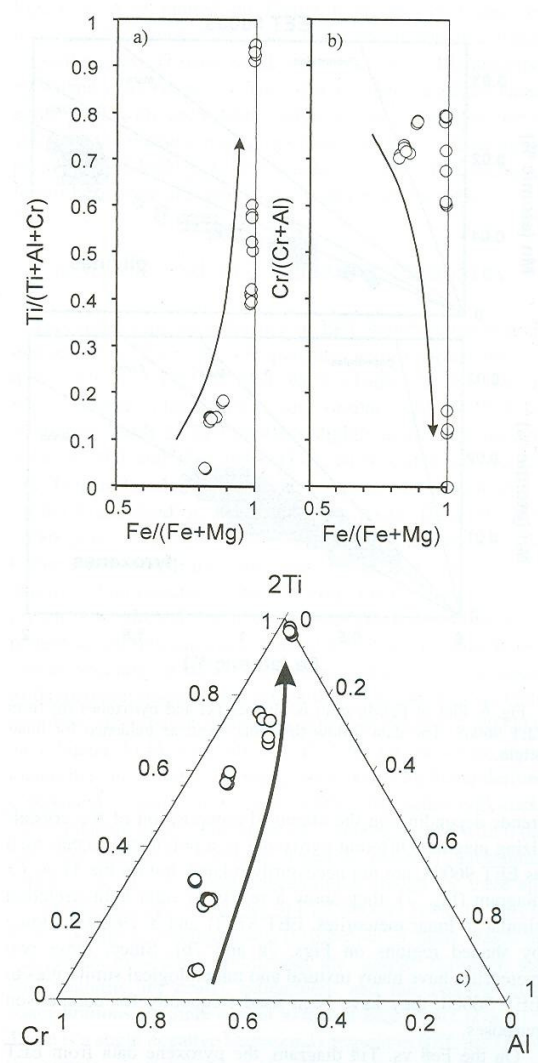

Figure 8: Spinel compositions for EET 96008 (Anand et al., 2003).

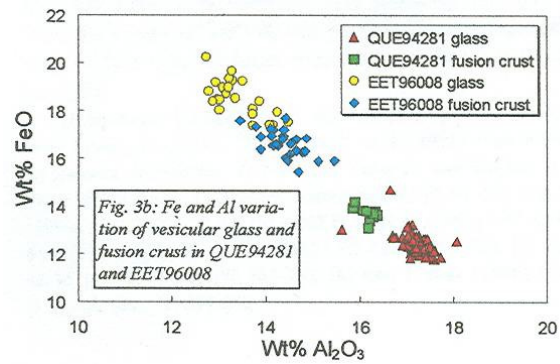

Figure 9: Composition of glass and fusion crust in EET 96008 compared to QUE 94281 (from Mikouchi et al., 2001)

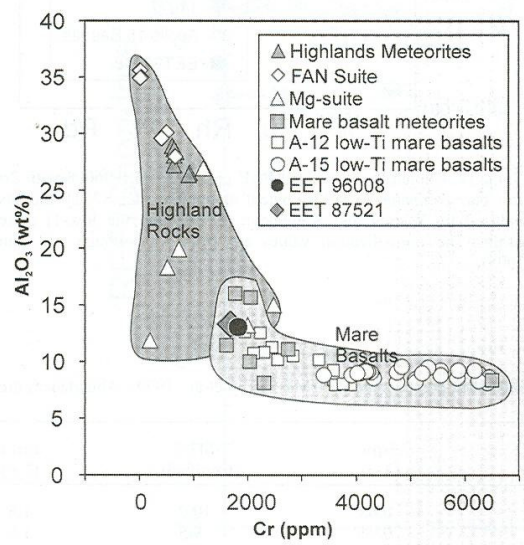

Figure 10: Bulk composition (Cr and Al_2O_3) for EET 96008 and EET 87521 compared to highland rocks and mare basalts (from Anand et al., 2003).

Chemistry

Numerous fractions of EET 87521 and EET 96008 have been analyzed by INAA and ICP-MS techniques (Table 1). A plot of Al_2O_3 vs. Cr shows that the EET meteorites plot at the intersection of the highlands and mare basalt fields. Their compositions are nearly identical, and very similar to many other lunar mare meteorites (Fig. 10). Analyses of glasses in EET 96008 illustrate their

basaltic nature compared to Al_2O_3-rich and FeO-poor glass analyses from highland breccia QUE 94281 (Fig. 9). Rare earth element data for EET 87521 and 96008 show the similarity to other mare basalts from Apollo and more basalt meteorites, given their distinct negative Eu anomalies, and elevated REE in general compared to highland meteorites (Fig. 11). Siderophile elements in EET 87521 and EET 96008 exhibit large concentration variations, typical of lunar breccias in general, such as Ir (Anand et al., 2003; Warren and Kallemeyn, 1991; Korotev et al., 2003). Variations between sub samples of EET 87521 and EET 96008 ca be attributed to the brecciated nature of the sample. Finally, noble gas abundance patterns for the EET meteorites show their similar, but relatively low concentrations of noble gases compared to highlands meteorite DaG 262 and solar noble gas-rich highland meteorite QUE 93069 (Fig. 12).

Radiogenic age dating

There has been no published Rb-Sr, Lu-Hf or Sm-Nd data for the EET meteorites.

There has been a U-Pb study of apatite and whitlockite from EET 96008, yielding an isochron of 3.69 Ga (Fig. 13), but with sizable error. Similar study of EET 87521 phosphates yielded age age of 3.531 Ga, in agreement (within error) of the results for EET 96008 (Fig. 14; Terada et al., 2005).

^{40}K-^{40}Ar gas retention ages for all phases in EET 87521 show a 3.30 Ga age (Eugster et al. (1996). This is in agreement with the results of Fernandes and Burgess (2006) who report a 3.23 Ga age for EET 96008. Fernandes et al. (2009) report 3.23 Ga age for the bulk, but a slight younger age (~2.7 Ga) for a basalt clast and slightly older age (~3.7 Ga) for the breccias (Fig. 15).

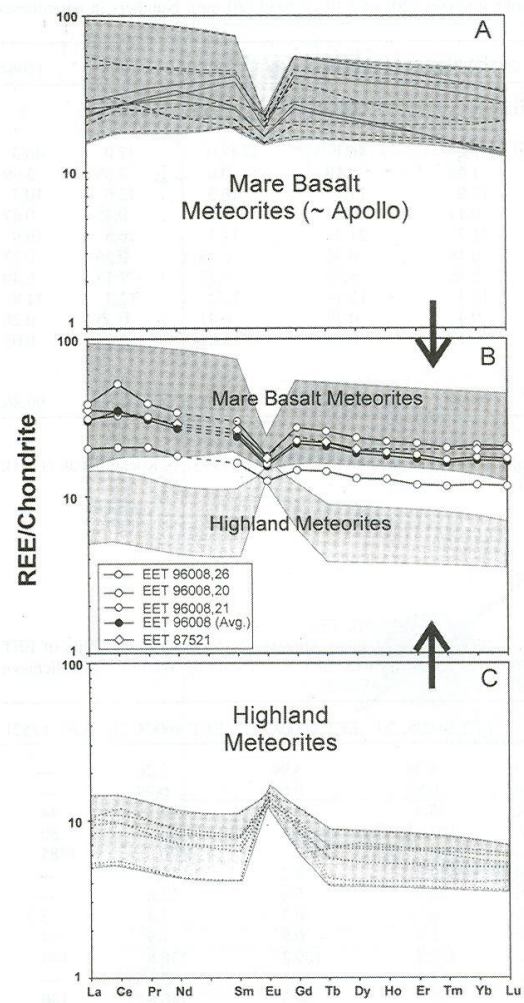

Figure 11: Rare earth element data for EET 87521 and 96008 illustrating the similarity of these meteorites to mare basalt.

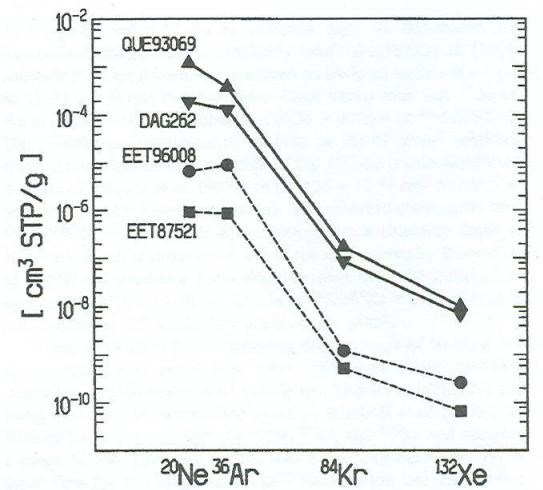

Figure 12: Noble gas data for EET 87521 and EET 96008 compared to two other lunar meteorites: QUE 93069 and DaG 262 (from Polnau and Eugster, 1999).

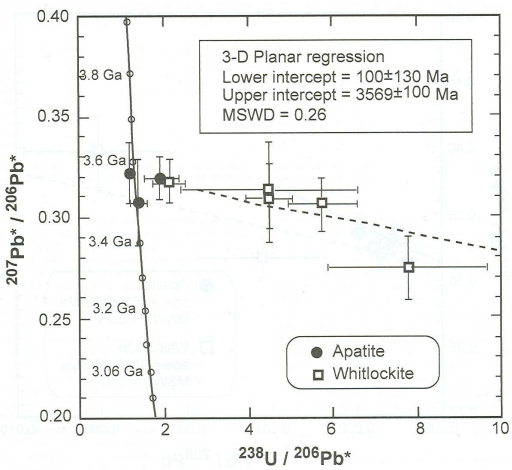

Figure 13: U-Pb data for apatite and whitlockite from EET 96008, illustrating the 3.569 Ga age (from Anand et al., 2003).

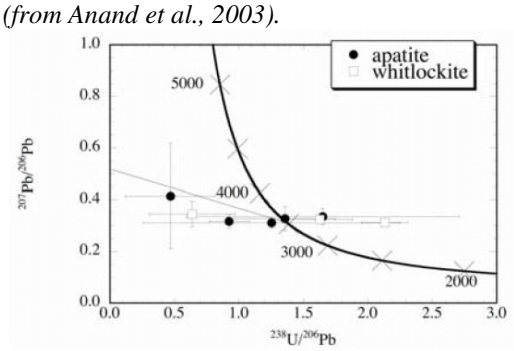

Figure 14: U-Pb data for apatite and whitlockite from EET 87521, illustrating the 3.531 Ga age (from Terada et al., 2005).

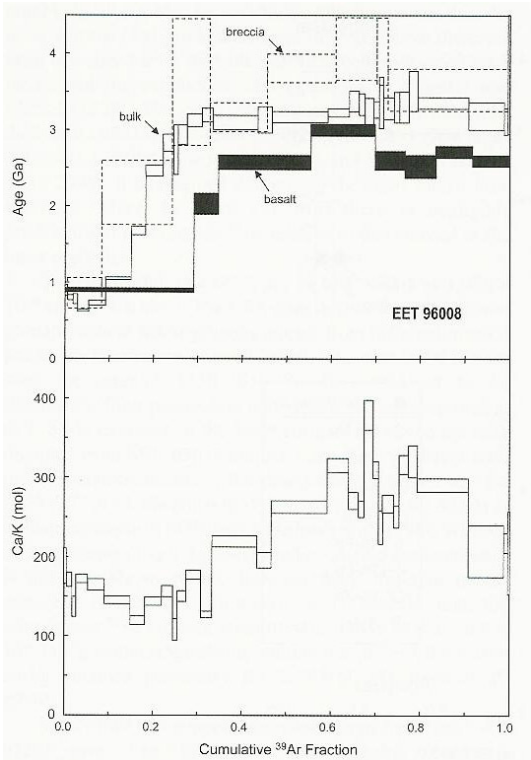

Figure 15: Ar-Ar ages and Ca/K ratios for EET 96008 bulk, basalt clast, and breccias portions (from Fernandes et al., 2009).

Cosmogenic isotopes, exposure ages

A summary of the ejection, transfer, and terrestrial exposure ages is presented in the introduction to this compendium. Only brief mention of detailed studies will be made here for the sake of brevity. Eugster et al. (2000) propose a three stage history for EET 96008: an early stage, ~500 Ma ago, lasting ~9 Ma at a shallow shielding depth, followed by the second stage when the material was buried (without exposure) until the third stage, where it was buried at an intermediate depth for about 26 Ma until ejection. This history is nearly identical to that proposed for EET 87521, and is solid basis for pairing of these two meteorites. Vogt et al. (1993) and Nishiizumi et al. (1999) demonstrate that the transit time of these meteorites from the Moon to the Earth was much less than 10 Ka, and the terrestrial residence time was 80 +/- 30 Ka.

Table 1a. Chemical composition of EET 87521 and EET 96008

reference	1	1	1	2	3	3
weight	,20	,21	,26		373.2	503.6
					87521	96008
method	b,d	b,d	b,d	e	b,e	b,e
SiO_2 %	46.5			47.9		
TiO_2	0.75			0.97		
Al_2O_3	13			13.2		
FeO	18.1			18.8	16.64	18.66
MnO	0.24			0.24		
MgO	7.72			6.79		
CaO	11.2			11.6	12.8	11.9
Na_2O	0.36			0.42	0.403	0.387
K_2O	0.05			0.06		
P_2O_5	0.07					
S %						
sum						
Sc ppm	45.4	40.8	46.7	44	34.2	37.2
V	103.4	128.2	97	80		
Cr	2530	1467	1470	1785	1827	1950
Co					45.7	48.9
Ni					80	60
Cu	9.2	8.2	10.7			
Zn	10.7	5.8	12.6			
Ga	6.7	6.3	7.4	5.3		
Ge						
As						
Se						
Rb	1.4	0.8	1.9	<4		
Sr	112.4	109.2	116.8	104	100	95
Y	33.4	26.4	39.8			
Zr	112	94.3	140.8	140	100	105
Nb	6.85	5	9.11			
Mo	0.12	0.09	0.1			
Ru						
Rh						
Pd ppb						
Ag ppb						
Cd ppb						
In ppb						
Sn ppb						
Sb ppb						
Te ppb						
Cs ppm	0.06	0.02	0.07	0.04	<0.2	<0.2
Ba	80.2	48.5	91.7	88	70	69
La	7.3	4.69	9.08	8.3	6.96	7.06

Ce	19.7	12.3	31.4	20.9	18	18.5
Pr	2.84	1.82	3.48			
Nd	12.7	8.12	15.4	13	12	11
Sm	3.65	2.38	4.42	3.86	3.41	3.43
Eu	0.9	0.7	1	0.98	0.84	0.8
Gd	4.42	2.88	5.38			
Tb	0.79	0.52	0.94	0.8	0.72	0.72
Dy	4.73	3.15	5.73	4.8		
Ho	1.05	0.71	1.24			
Er	2.89	1.87	3.42			
Tm	0.41	0.28	0.49			
Yb	2.86	1.92	3.4	3.19	2.55	2.6
Lu	0.42	0.28	0.5	0.48	0.35	0.363
Hf	2.42	1.7	3.02	2.88	2.57	2.62
Ta	0.34	0.22	0.55	0.37	0.3	0.3
W ppb	180	90	210			
Re ppb						
Os ppb						
Ir ppb					<8	<7
Pt ppb						
Au ppb					<9	<8
Th ppm	0.82	0.51	1.1	0.95	1	0.9
U ppm	0.3	0.19	0.35	0.23	0.28	0.21

technique (a) ICP-AES, (b) ICP-MS, (c) IDMS, (d) FB-EMPA, (e) INAA, (f) RNAA

Table 1b. Light and/or volatile elements for EET 87521 and EET 96008

Li ppm	4.39	3.99	5.26
Be	0.82	0.6	0.99
C			
S			
F ppm			
Cl			
Br			
I			
Pb ppm	0.8	0.24	0.99
Hg ppb			
Tl			
Bi			

References: 1) Anand et al., (2003); 2) Warren and Kallemeyn (1991); 3) Korotev et al. (2003).

Processing

EET 87521 was processed in two main stage: initial processing between June 1988 and February 1990, until it was recognized as a lunar meteorite and then between March and August 1990 when it was studied by consortium including C. Schwarz, J.S. Delaney, P. Warren, and M. Lindstrom (Figure 16,17,20). Most allocations to scientists have been from ,0 and ,11 (Table 2). EET 96008 was also processed in two main stages: initial processing in April 1997 and then most allocations in July 1998 (Figure 18, 19, 21). Most of the allocations have been from ,3 and ,0 (Table 3).

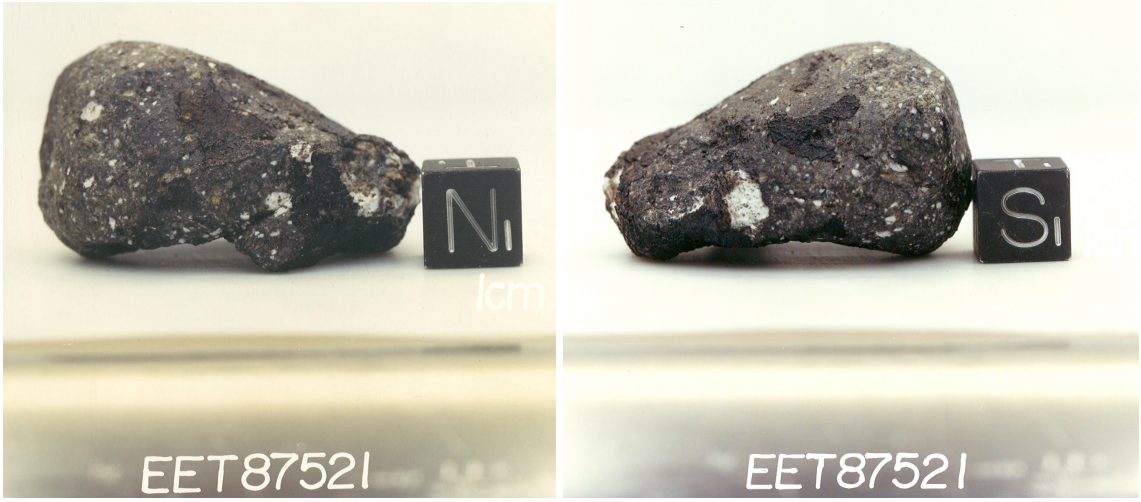

Figure 16: Two different views of EET 87521 in the meteorite processing laboratory at JSC. Scale cube is 1 cm in all photos.

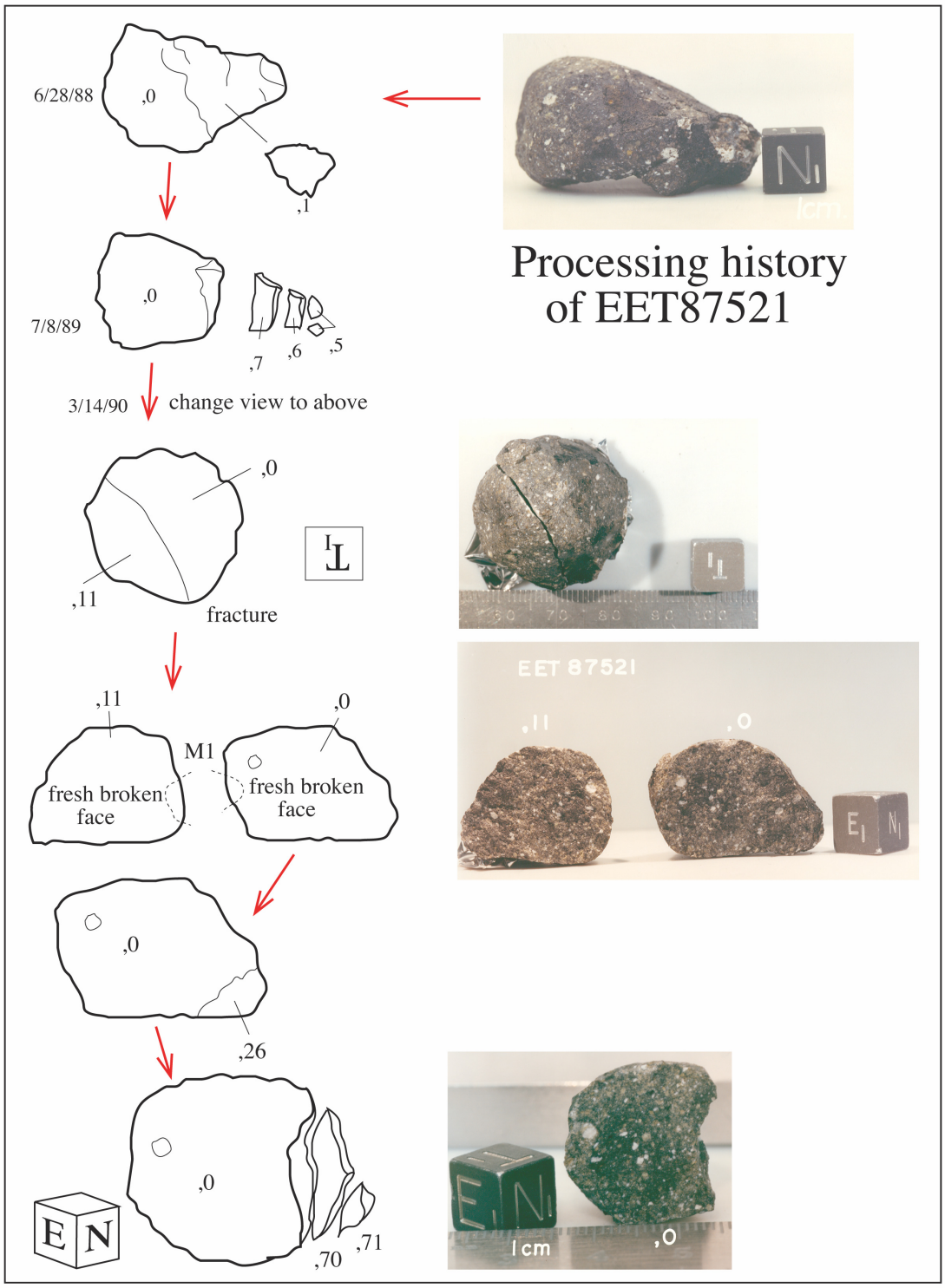

Figure 17: Photographs and sketches of processing of EET 87521.

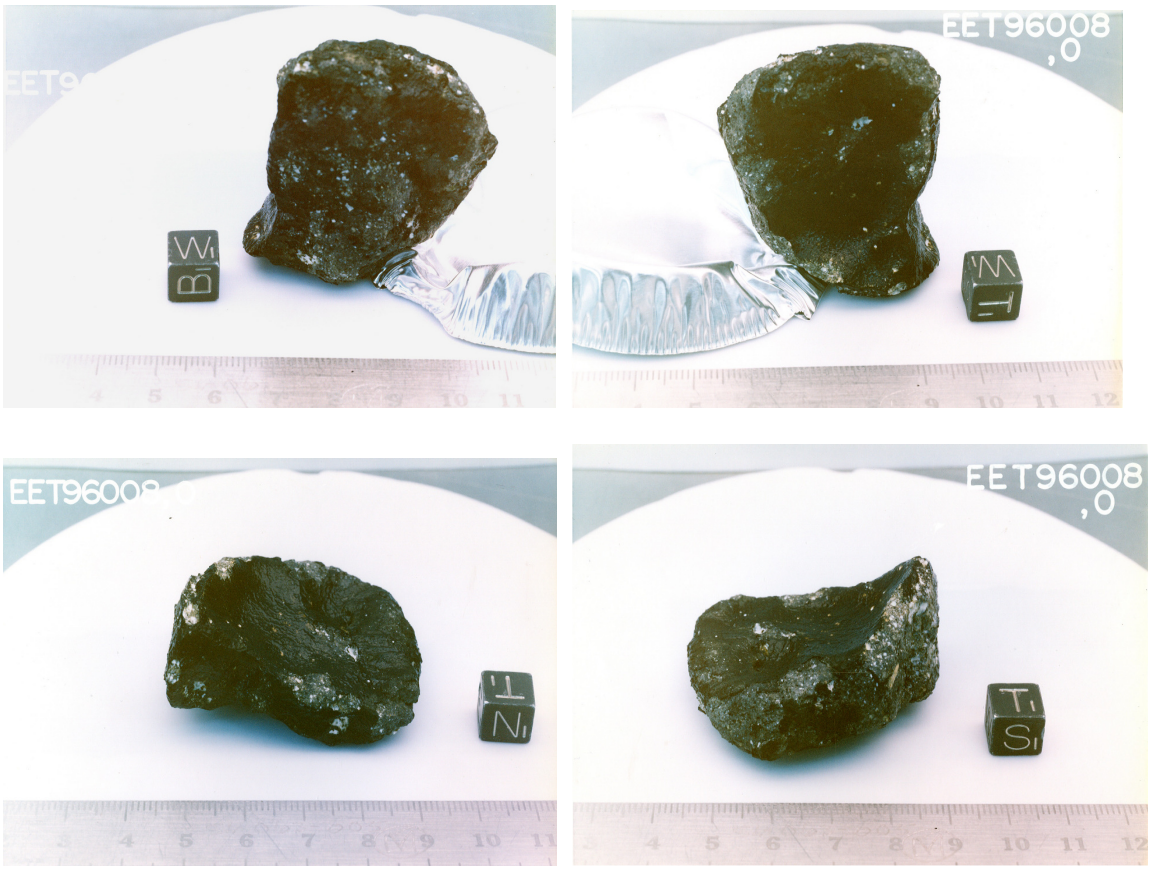

Figure 18: Four different views of EET 96008 in the meteorite processing laboratory at JSC. Scale cube is 1 cm in all photos.

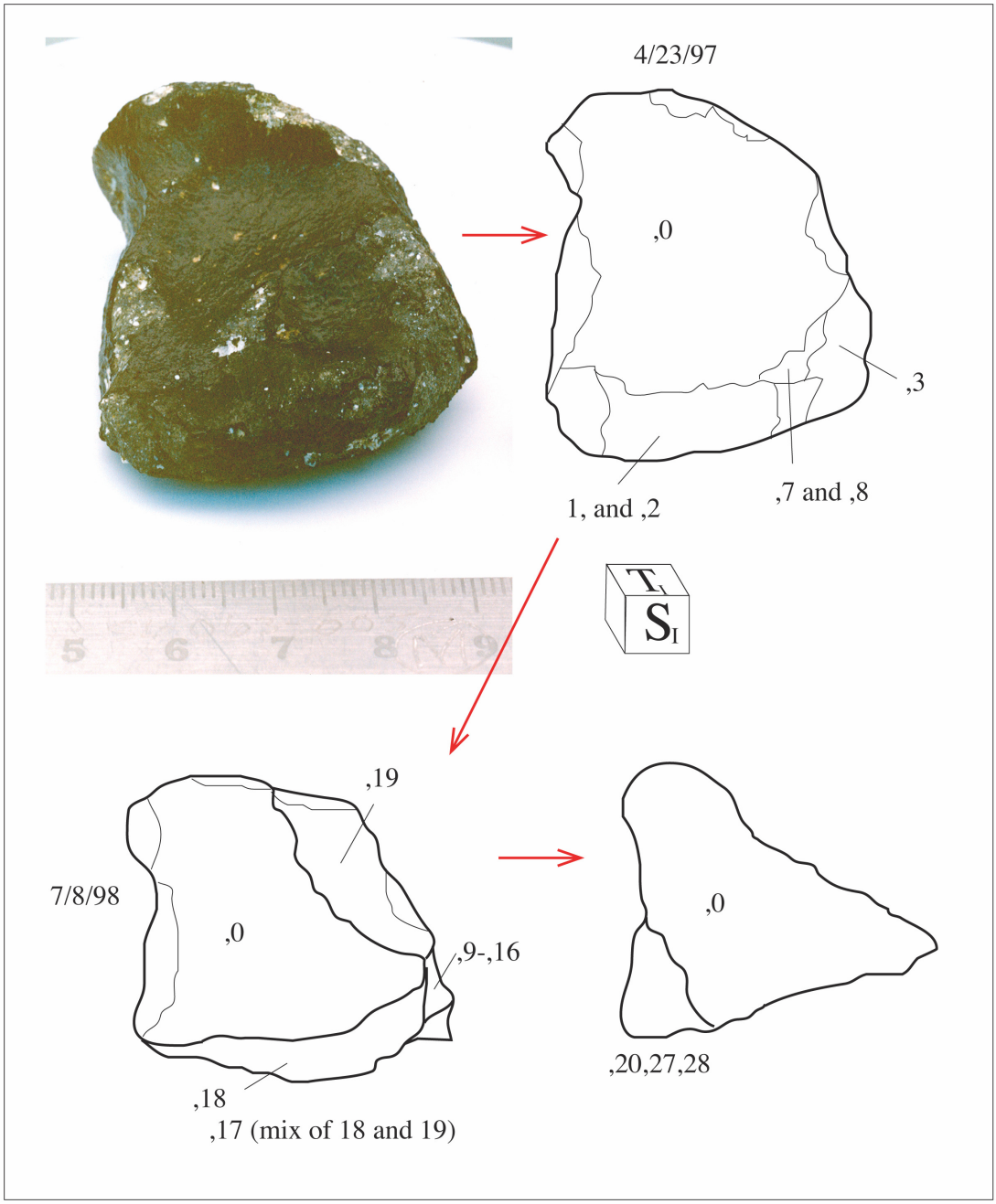

Figure 19: Photographs and sketches of processing of EET 96008.

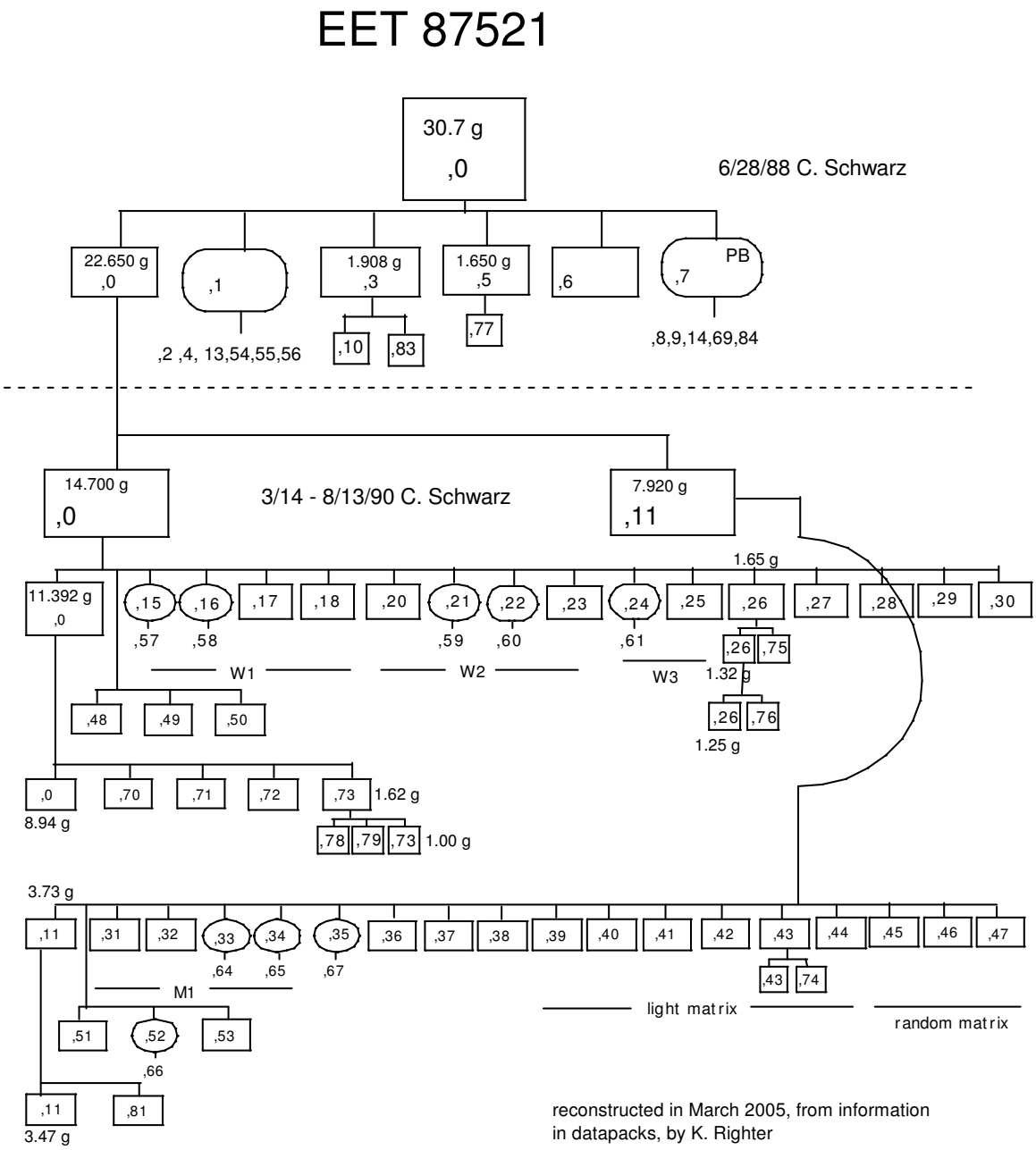

Figure 20: Genealogy diagram of EET 87521, based on information in datapacks for this meteorite.

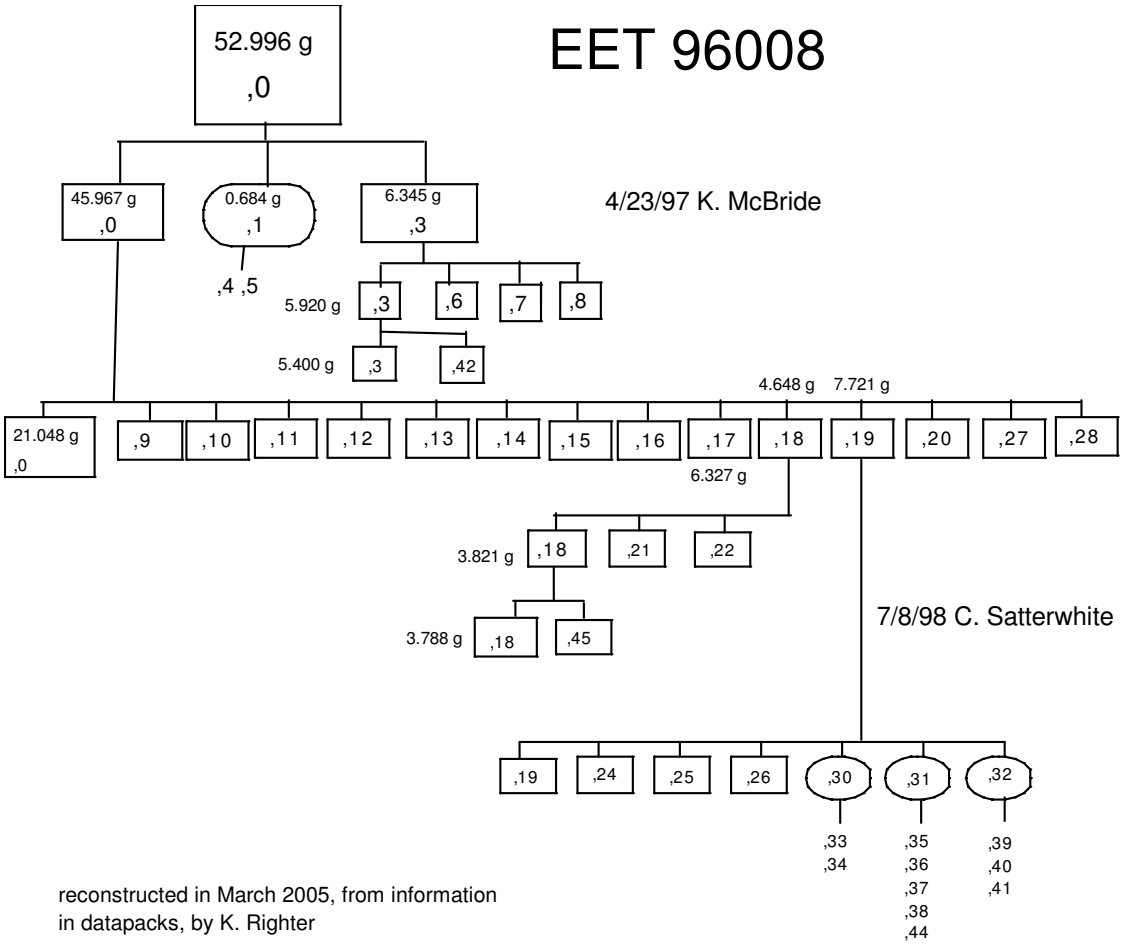

Figure 21: Genealogy diagrams of EET 96008, based on information in datapacks for this meteorite.

Table 2: Allocation history of EET 87521

SPLIT	parent	TS	WEIGHT	LOCATION	DESCRIPTION
0			8.94	JSC	doc cp
1	0		1.826	JSC	potted butt
		2	0.01	Terada	thin section
		4	0.01	SI	library thin section
		13	0.01	JSC	thin section
		54	0.01	Barsukov	thin section
		55	0.01	Arai	thin section
		56	0.01	JSC	thin section
3	0		1.813	JSC	cps + fines
5	0		1.58	JSC	cps
6	0		0.6	Wasson	interior chip
7	0		1.9	JSC	potted butt
		8	0.01	Delaney	thin section

		9	0.01	Wasson	thin section
		14	0.01	Stöffler	thin section
		69	0.01	Warren	thin section
		84	0.01	JSC	thin section
10	3		0.015	Clayton	interior chip
11	0		3.47	JSC	cps + fines
15	0		entirely subdivided		potted butt
		57	0.005	Delaney	thin section
16	0		0.071	JSC	potted butt
		58	0.01	Delaney	thin section
17	0		0.011	Warren	W1 + matrix
18	0		0.004	Warren	W1 cps
19	0		0.022	Delaney	dust W/W1
20	0		0.01	Warren	W2 cps
21	0		0.054	JSC	potted butt
		59	0.01	Delaney	thin section
22	0		0.052	JSC	potted butt
		60	0.01	Delaney	thin section
23	0		0.007	Delaney	dust W/W2
24	0		entirely subdivided		potted butt
		61	0.01	Delaney	thin section
25	0		0.008	JSC	W3 dust
26	0		1.286	JSC	cps + fines
27	0		0.018	Warren	M2 cps
28	0		0.095	JSC	potted butt
		62	0.01	Delaney	thin section
29	0		0.127	JSC	potted butt
		63	0.01	Delaney	thin section
30	0		0.024	JSC	dust W/M2
31	11		0.038	Warren	M1 cl cp
32	11		0.009	Warren	M1 cl cps
33	11		0.081	JSC	potted butt
		64	0.01	Delaney	thin section
34	11		0.085	JSC	potted butt
		65	0.01	Delaney	thin section
35	11		0.258	JSC	potted butt
		67	0.01	Delaney	thin section
36	11		0.025	Sears	light matrix chip
37	11		0.05	Lindstrom M	light matrix chip
38	11		0.155	Eugster	light matrix chip
39	11		0.322	Eugster	dark matrix chip
40	11		0.051	Sears	dark matrix chip
41	11		0.151	Lindstrom M	dark matrix chip
42	11		0.134	Lindstrom M	dark matrix chip
43	11		0.032	JSC	interior dark matrix
44	11		0.657	JSC	exterior dark matrix
45	11		0.028	Takeda	chips

46	11		0.364	Palme	matrix chips
47	11		1.219	Barsukov	exterior matrix chips
48	0		0.245	Nishiizumi	interior locatable chip
49	0		0.244	Herzog	2 interior locatable chips
50	0		0.583	JSC	locatable chips
51	11		0.106	JSC	dark matrix chip
52	11		0.232	JSC	potted butt
		66	0.01	Delaney	thin section
53	11		0.125	JSC	chips
70	0		0.504	Jull	interior chip
71	0		0.098	Grady	interior chip
72	0		0.227	Herzog	interior chip
73	0		1.002	JSC	chips + fine
74	43		0.03	Dyar	interior chip
75	26		0.333	Delaney	interior chip
76	26		0.03	Miyamoto	interior chips
77	5		0.07	Vogt	interior chip
78	73		0.351	Ebihara	interior chips
79	73		0.209	Korotev	interior chips
81	11		0.18	Korotev	interior chips
83	3		0.08	Zolensky	chip with fusion crust

Table 3: Allocation history of EET 96008

SPLIT	parent	TS	WEIGHT	LOCATION	DESCRIPTION
0			21.048	JSC	doc piece
1	0		0.664	JSC	potted butt
		4	0.01	SI	thin section
		5	0.01	JSC	library thin section
3	0		5.4	JSC	cps + fines
6	3		0.064	Lindstrom M.	white clasts
7	3		0.128	Korotev	chip with fusion crust
8	3		0.203	Nishiizumi	fusion crust
9	0		0.299	Lindstrom M.	clast chips
10	0		0.95	Lindstrom M.	matrix chips
11	0		0.217	Nishiizumi	fusion crust, chip B side
12	0		0.14	Nishiizumi	interior chip
13	0		0.438	Warren	S face chip
14	0		0.245	Korotev	interior chips
15	0		0.296	Ebihara	interior chip
16	0		0.063	Mikouchi	interior chips
17	0		6.327	JSC	cps + fines
18	0		3.788	JSC	S face chips
19	0		3.308	JSC	N face chips
20	0		0.161	Snyder	2 interior chips
21	0		0.172	Snyder	interior chips

22	0		0.595	Eugster	interior chip
24	0		0.256	Korotev	interior chips
25	0		0.376	Warren	interior chip
26	0		0.151	Snyder	interior chip
27	0		1.024	Dreibus	interior chips
28	0		2.219	JSC	cps
30	19		0.9	JSC	potted butt
		33	0.01	Korotev	thin section
		34	0.01	Keil	thin section
31	19		1.75	JSC	potted butt
		35	0.01	Mikouchi	thin section
		36	0.01	Stöffler	thin section
		37	0.01	Warren	thin section
		38	0.01	Snyder	thin section
		44	0.01	JSC	thin section
32	19		0.88	JSC	potted butt
		39	0.01	Snyder	thin section
		40	0.01	JSC	thin section
		41	0.01	Miyamoto	thin section
42	3		0.491	Jull	2 interior chips
45	18		0.021	Bizarro	chip